Thermochimica Acta 491 (2009) 80–83

Contents lists available at ScienceDirect

Thermochimica Acta

journal homepage: www.elsevier.com/locate/tca

Heat capacity of $NaNO_2$

L. Kourkova[a,*], R. Svoboda[b], G. Sadovska[a], V. Podzemna[a], A. Kohutova[a]

[a] Department of Inorganic Technology, Faculty of Chemical Technology, University of Pardubice, Pardubice, Czech Republic
[b] Department of Physical Chemistry, Faculty of Chemical Technology, University of Pardubice, Pardubice, Czech Republic

ARTICLE INFO

Article history:
Received 5 January 2009
Received in revised form 3 March 2009
Accepted 6 March 2009
Available online 20 March 2009

Keywords:
Sodium nitrite
Heat capacity
Enthalpy
Phase change materials
Calorimetry

ABSTRACT

Heat capacity in solid state was for the sodium nitrite ($NaNO_2$) measured by using two types of calorimeters. The measurements were performed in the temperature range 273.15–583.15 K. Three phase changes were observed in this temperature range – one melting and two transitions between different structural modifications. Concerning the transitions between structural modifications, the first was observed at 437.2 ± 0.1 K and the second was found at 438.7 ± 0.1 K. Temperature of melting was then determined to be 553.2 ± 0.2 K with the corresponding heat of fusion being equal to 13.9 ± 0.1 kJ mol^{-1}.

1. Introduction

Storage of available thermal energy is very important in many engineering applications. Latent heat storage is one of the most efficient ways of storing thermal energy [1]. This technique is based on the storing and releasing of thermal energy by a substance during its phase transition. Nowadays, the most frequently exploited phase changes are the solid–solid (between different modifications) and solid–liquid (melting, crystallization) transitions. Knowledge of heat capacity and enthalpy change during the considered transition is then necessary for the calculation of energy amount that can be stored in the substance. Besides the desired high values of heat capacity and enthalpy change during the transition also several other important parameters have to be taken into account for the heat storage applications – i.e. suitable temperature of the phase transition, long term stability under thermal cycling without traces of supercooling or phase segregation, high thermal conductivity, low reactivity, price etc.

Sodium nitrite belongs to a group of phase change materials (PCMs) and as such might find utilization in high temperature range energy storage applications (e.g. in solar power plants). $NaNO_2$ melts at ~553 K [2–4] while other two phase transitions can be found near 437 K in solid state [5–11]. The first transition is related to a change from the ferroelectric phase to the sinusoidal antiferroelectric phase at the Curie temperature (T_C). During the second transition the sinusoidal antiferroelectric phase changes to the paraelectric one at the Neél temperature (T_N). A summary of Curie and Neél temperatures published by several authors is reported in Table 1.

Heat capacity and enthalpy of phase transitions were for $NaNO_2$ reported by Sakiyama et al. [5] in the temperature range 275–468 K. Similar heat capacity measurements were carried out by Hoshino [12] in the narrow temperature interval near the two solid–solid transitions. Heat capacity in the temperature range 300–475 K with an emphasis on the solid–solid transitions region is published in the papers of Hatta et al. [10–11]. In the work of Kamimoto [2] and Cases [3] calorimetric measurements were performed to determine the heat of fusion and heat capacity of liquid $NaNO_2$. Both solid–solid transitions have been also studied by using various other experimental techniques: X-ray diffraction [13–15], spectroscopic methods [8,16–18], dielectric measurements [9,19–21].

In this work the results of our calorimetric study focused on the determination of heat capacity for $NaNO_2$ in a wider range of temperatures (i.e. from 273.15 K up to the melting temperature of the sample) are presented. The temperature dependence of heat capacity is then used for calculation of enthalpy and entropy changes. The enthalpy of fusion was also determined. In the second part of the paper a detailed study of the two nearby phase transitions that occur in solid $NaNO_2$ will be presented.

2. Experimental details

2.1. $NaNO_2$ and its characterization

The sodium nitrite was of an analytical reagent grade ($NaNO_2$ content ~99.8%). Sample was oven-dried at 393.15 K for 24 h and

* Corresponding author. Tel.: +420 466 037 173.
E-mail address: lucie.kourkova@upce.cz (L. Kourkova).

0040-6031/$ – see front matter © 2009 Elsevier B.V. All rights reserved.
doi:10.1016/j.tca.2009.03.005

Table 1
Curie temperatures (T_C) and Neél temperatures (T_N) for $NaNO_2$.

	Calorimetric study [5]	Calorimetric study [7]	Spectroscopic study [8]	Dielectric study [9]	Calorimetric study [11]
T_C	436.55	436.1 ± 1.1	436.3	436.85	436.75
T_N	437.15	437.3 ± 1.3	437.7	438.35	437.95

stored in a desiccator. X-ray diffraction data of the sample were obtained at 298.15 K for CuKα radiation by using the D8-Advance diffractometer (Bruker AXE, Germany) and secondary graphite monochromator The X-ray diffraction confirmed orthorhombic, body-centred lattice with the parameters $a = 3.5726 \pm 0.0010$ Å, $b = 5.5835 \pm 0.0012$ Å and $c = 5.4015 \pm 0.0012$ Å. The lattice parameters are in a good agreement with tabulated data [22].

2.2. Methods of measurement

Two differential scanning calorimeters, DSC Pyris 1 (PerkinElmer, USA) and DSC 822^e (Mettler, USA), and a C80 calorimeter (Setaram, France) were used for experimental measurements. The following description of particular measurements is sorted out with respect to the device the measurement was performed by.

Heat capacity plus respective enthalpies of fusion and of the two solid–solid transitions were measured by using the DSC Pyris 1 in the temperature range 273.15–583.15 K. Melting temperatures of pure metals (Hg, Ga, In, Sn, Pb) and enthalpy of fusion of In were used to calibrate the calorimeter. Heat capacity measurements were performed at heating rate 5 K min^{-1}, the sample masses were approximately 10 mg. In order to separate the two nearby solid-solid transitions an additional measurement was performed at heating rate 0.5 K min^{-1} in the temperature range 420.15–440.15 K. Heat capacity was from the measurements determined by the so called ratio method [23], this procedure required one additional measurement with a standard material (sapphire in our case) at the same heating rate as was that of the original sample measurement. Accuracy of heat capacity measurements was tested by measuring molybdenum (NIST Standard reference material No. 781D2) in the temperature range 293.15–573.15 K. The accuracy was for the DSC Pyris 1 estimated to be better than 2%. The precision of heat capacity measurements was determined from five reproduced curves and was found to be better than ±2.5%. All measurements described in this paragraph were performed under the dry nitrogen atmosphere (20 cm^3 min^{-1}).

In addition, several heat capacity measurements were also performed using the C80 heat conduction differential calorimeter. In this case the temperature range was limited by the device construction to 303.15–563.15 K. The sample mass was approximately 7 g. Heat capacity was from the measurements determined by the so called increment method at heating rate 0.5 K min^{-1}. Details of the method are described elsewhere [24]. Synthetic sapphire (NIST Standard reference material no. 720) was used as the reference material. The accuracy of heat capacity measurements was found to be better than 2% in the studied temperature range. The precision of heat capacity measurements was for Setaram C80 determined from three reproduced curves and was found to be better than ±2%. The calorimeter was calibrated electrically using the Joule-effect calibration unit supplied by Setaram.

Finally, the DSC 822^e was used to study the two solid-solid transitions. This was done due to the DSC 822^e having much better stability and reproducibility at very low cooling rates than the DSC Pyris 1 (the low cooling rates were fundamental in order to fully separate the two nearby transitions). The DSC 822^e was calibrated by using the melting temperatures of pure metals (Ga, In, Zn) and the enthalpy of fusion of In. Mass of each sample was approximately 10 mg and dry nitrogen was used as the purge gas at a rate of 20 cm^3 min^{-1}.

3. Results and discussion

The experimental values of molar heat capacity obtained for $NaNO_2$ from the DSC Pyris 1 and C80 measurements are available as Supplementary Material (the introduced DSC data were acquired at heating rate 5 K min^{-1}). These data are shown in Fig. 1 together with values obtained by Sakiyama et al. [5]. Taking a look at our data, the maximum difference between the C_p values obtained by DSC and C80 was observed at 403.15 K, where the C80 values were by approximately 4% lower than those obtained by DSC. Origin of this divergence may lie in the fact that different methods of C_p evaluation (ratio vs. increment) and different sample masses (masses in the order of few milligrams in the case of DSC vs. several grams of sample in the case of C80) were used in each case. However, the precision envelopes of heat capacity measurements performed by both instruments at least partially superpose, thus the difference lies within the statistical error. If we compare our data to those of Sakiyama, one can see that his C_p values are approximately 15–19% lower than our data. The reason for this is unknown to us so far, its origin may possibly lie in different purities of the material or maybe in a slightly inaccurate calibration of the Sakiyama's calorimeter (the calibration process is unfortunately not described in [5]). The heat capacity data obtained by AC calorimetry and published by Hatta et al. [10] are not shown in the Fig. 1 because no discrete values are unfortunately given in that paper. However, after digitizing the data from Fig. 2 in [10] and shifting the origin of their ordinate (according to what is described in [11]; the procedure is a form of correction due to the exclusion of additional heat capacity associated with the thermocouple and glue attached to the sample during ACC measurements) we could see that the C_p data published by Hatta are in a good agreement with our values. The difference between the two dependencies was approximately 2% (Hatta's data being lower).

The experimental molar heat capacities obtained by DSC were fitted using a polynomial function (Eq. (1)). This was done in two separate temperature regions (due to the presence of the phase transitions), the first temperature range being 273.15–408.15 K and the second 463.15–530.15 K, respectively. These temperature

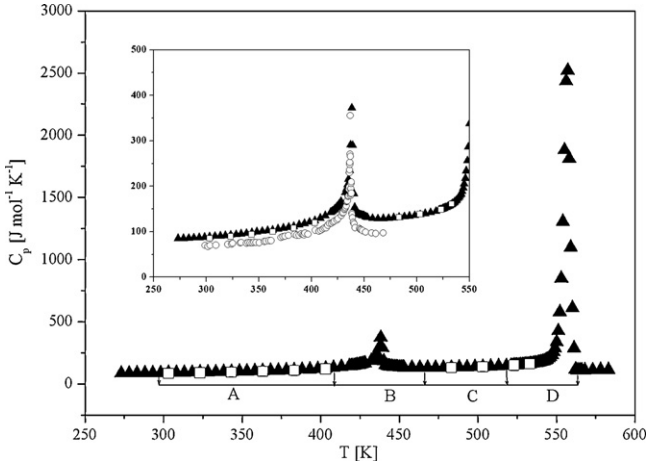

Fig. 1. Heat capacity of $NaNO_2$: (▲) DSC Pyris 1; (□) Setaram C80; (○) Ref. [5]; heating rate 5 K min^{-1}. The heat capacity data are divided into four temperature intervals. Inset shows the heat capacity data zoomed in the solid state region.

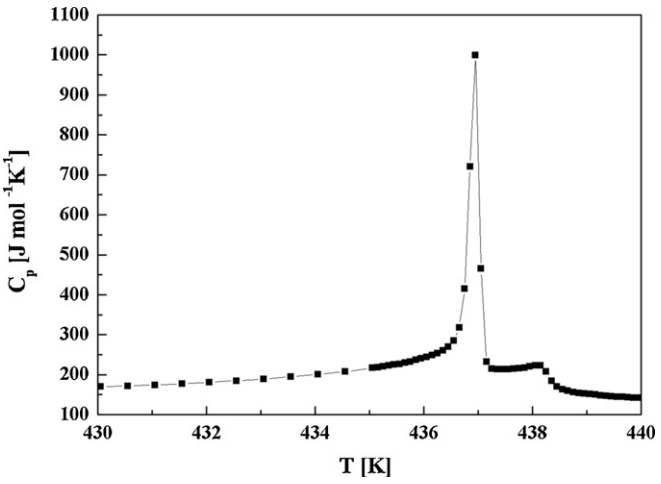

Fig. 2. Heat capacity of the first and second phase transition of $NaNO_2$ measured by DSC Pyris 1 (0.5 K min^{-1}).

regions were chosen to be the widest possible while still having the correlation coefficient of the resulting fit $R^2 \approx 0.995$ (in order not to include the data points that are too close to the present transitions and therefore were not reproducible under different cooling/heating rates). Final parameters of both polynomial equations are listed in Table 2 (the confidence intervals were calculated as $\pm 1\sigma$).

The calculation of the energy accumulated in the temperature interval studied in this paper can be then done according to the Fig. 1 and Eq. (2). The heat capacity data are in the Fig. 1 divided into four regions A–D, where the regions A and C are the two above mentioned and fitted C_p plateaus, the regions B and D are then the temperature intervals covering the solid–solid transitions and fusion, respectively. Accumulated heat is then given by the Eq. (2), where n is the amount of substance and particular terms in brackets stand for the enthalpy changes in the corresponding temperature regions (according to the subscripts). The enthalpy changes in regions A and C were calculated from the temperature dependence of heat capacity according to the integrals in Eq. (2) (more generally according to Eq. (3)) and are available as Supplementary Material. In addition, the entropy changes were for the two regions calculated according to the Eq. (4). The behaviour of heat capacity in regions B and D partially depends on the conditions of the measurement and therefore it is correct (based only on non-isothermal measurements) to give just the values of the total enthalpy contributions: $q_B = 8.706$ J mol^{-1} and $q_D = 18.100$ J mol^{-1}.

$$C_p = P_1 + P_2T + P_3T^2 \quad (1)$$

$$Q = n\left[\int_{298.15}^{408.15} C_{pA}(T)dT + q_B + \int_{463.15}^{530.15} C_{pC}(T)dT + q_D\right] \quad (2)$$

$$\Delta H = H_{T2} - H_{T1} = \int_{T1}^{T2} C_p(s)dT \quad (3)$$

Table 2
Parameters (P_1, P_2, P_3) and coefficient of determination (R^2) of the polynomial function (Eq. (1)) used to fit the heat capacity data.

Parameters	Temperature interval (K)	
	273.15–408.15	463.15–530.15
P_1	237 ± 15	1469 ± 97
P_2	-1.128 ± 0.086	-5.75 ± 0.39
P_3	$(2.10 \pm 0.12) \times 10^{-3}$	$(6.17 \pm 0.39) \times 10^{-3}$
R^2	0.9947	0.9959

$$\Delta S = S_{T2} - S_{T1} = \int_{T1}^{T2} \frac{C_p(s)}{T}dT \quad (4)$$

As was already mentioned, two nearby phase transitions occur in the solid $NaNO_2$. A detailed study of these phase transformations will be presented in the following paragraph. Unfortunately, due to the thermal gradients resulting from the large mass of the sample used in the calorimeter C80, only a single peak with a shoulder was observed, using this instrument, even for the lowest applied heating rate. On the other hand, by using the DSCs both transformations were fully distinguished. Basic thermal characterization of the sample was primarily carried out by using the DSC 822^e due to its better stability at slow cooling rates (when compared to the DSC Pyris 1). The corresponding values obtained from measurements performed on the DSC Pyris 1 will be therefore given in parentheses. The measurements on both instruments were performed repeatedly at cooling rates 0.2, 0.5 and 1 K min^{-1}. Results are given as mean values out of 10 measurements. The onset on cooling of the first order transition was observed at 437.18 ± 0.06 (437.04 ± 0.16) K and the corresponding enthalpy of the effect was found to be $\Delta H = 327.3 \pm 4.8$ (318 ± 14) J mol^{-1}. Midpoint of the second order transition was then observed at 438.74 ± 0.05 (438.76 ± 0.13) K and the corresponding change of heat capacity was determined to be $\Delta C_p = 99.4 \pm 5.5$ (91.1 ± 2.8) J mol^{-1} K^{-1}. If the results of both DSCs are compared, one can see that the absolute values are very close; however the precision of the measurements is for the DSC 822^e much higher. If we compare our results with literature (summarized in Table 1), it can be said that our values of T_N and T_C are very close to those published, however, slight divergences can be found. Their origin can be assigned to different measurement techniques and sample masses, but above all to dissimilar methods of T_N and T_C evaluation (e.g. the difference between the evaluation from cooling and heating). When we tried to compare our value of enthalpy of the first order transition with literature, we found that only two papers with this value are at disposal. The first paper was published by Sakyiama et al. [5], who divided their studied temperature range into four stages. The first stage ranged from 333.15 K to 436.55 K with the corresponding enthalpy 1.584 kJ mol^{-1}. After the first stage two narrow temperature intervals (436.55–437.15 K and 437.15–438.15 K) followed, each with enthalpy equal to 234.08 J mol^{-1}. The last, fourth stage ranges from 438.15 to 459.15 K; the corresponding enthalpy was 163.02 J mol^{-1}. However, it is very important to mention, that Sakiyama evaluated enthalpy of these four stages as if all four were only parts of one large effect, that is that the baseline for evaluation was extrapolated from 333.15 to 459.15 K. Therefore no comparison with our data could be made. The second paper dealing with phase transition enthalpies was published by House and Goerne [7]. For the first order transformation they determined the value of $\Delta H = 249 \pm 5$ J mol^{-1}, while our value is approximately 1.3× higher. This discrepancy might be caused by improper evaluation due to the incomplete separation of the two effects (the cooling rates applied by House were 1, 2 and 4 K min^{-1}). In addition, House also evaluated enthalpy change of the second order transition equal to 27 ± 3 J mol^{-1}; in our opinion it would be more correct to characterize the second order transition by using ΔC_p.

Furthermore, in order to determine heat capacity in the very vicinity of the two transitions more accurately, a measurement at heating rate 0.5 K min^{-1} was performed in the temperature range 420.15–440.15 K using the DSC Pyris 1 (Fig. 2; the heat capacity data are available as Supplementary Material).

Melting point investigated by the DSCs was detected at 553.2 ± 0.2 (553.8 ± 0.2) K and the corresponding heat of fusion was 13.87 ± 0.14 (13.94 ± 0.21) kJ mol^{-1}. As the enthalpy change associated with the 530.15 to 564.15 temperature increase was found to be 18.1 kJ mol^{-1}, the direct contribution of fusion generates ~77%

of this value (the remainder originates from the C_p correction in the given temperature range). The heat of fusion presented in this work is close to the value 15.3 kJ mol^{-1} published by Kamimoto [2] and 14.9 ± 0.8 kJ mol^{-1} introduced by Cases [3]. Based on the high values of heat capacity and enthalpy of fusion, it can be concluded that $NaNO_2$ seems to be a promising material for thermal energy storage applications.

Acknowledgement

The financial support of the Czech Ministry of Education, Youth and Sports, research project MSM 0021627501 is gratefully acknowledged.

Appendix A. Supplementary data

Supplementary data associated with this article can be found, in the online version, at doi:10.1016/j.tca.2009.03.005.

References

[1] M.F. Demirbas, Energy Source 1 (2006) 85.
[2] M. Kamimoto, Thermochim. Acta 41 (1980) 361.
[3] J.C. Cases, Rev. Chim. Miner 10 (1973) 577.
[4] A. Fokin, Y. Kumzerov, E. Koroleva, A. Naberezhnov, O. Smirnov, M. Tovar, S. Vakhrushev, M. Glazman, J. Electroceram. 22 (2009) 270.
[5] M. Sakiyama, A. Kimoto, S. Seki, J. Phys. Soc. Jpn. 20 (1965) 2180.
[6] S. Tanisaki, J. Phys. Soc. Jpn. 16 (1961) 579.
[7] J.E. House, J.M. Goerne, Thermochim. Acta 215 (1993) 297.
[8] H. Yurtseven, I.E. Caglar, Spectrochim. Acta A 58 (2002) 55.
[9] K. Ema, K. Hamano, H. Maruyama, J. Phys. Soc. Jpn. 57 (1988) 2174.
[10] I. Hatta, A. Ikushima, J. Phys. Chem. Sol. 34 (1973) 57.
[11] I. Hatta, H. Ichikawa, M. Todoki, Thermochim. Acta 267 (1995) 83.
[12] S. Hoshino, J. Phys. Soc. Jpn. 19 (1964) 140.
[13] S. Tanisaki, J. Phys. Soc. Jpn. 18 (1963) 1181.
[14] Y. Yamada, I. Shiubya, S. Hoshino, J. Phys. Soc. Jpn. 18 (1963) 1594.
[15] S. Hoshino, H. Motegi, Jap. J. Appl. Phys. 6 (1967) 708.
[16] W. Buchheit, G. Herth, J. Peterson, Solid State Commun. 40 (1981) 411.
[17] A. Takase, K. Miyakawa, J. Phys. C Solid State 18 (1985) 5579.
[18] M.A. Fahim, Thermochim. Acta 363 (2000) 121.
[19] S. Sawada, S. Nomura, S. Fujii, I. Yoshida, Phys. Rev. Lett. 1 (1958) 320.
[20] K. Hamano, J. Phys. Soc. Jpn. 19 (1964) 945.
[21] B. Wyncke, F. Brehat, G.V. Kozlov, Phys. Status Solidi B 129 (1984) 531.
[22] F.H. Allen, Acta Cryst. B 58 (2002) 380.
[23] M.J. O'Neill, Anal. Chem. 38 (1966) 1331.
[24] L. Kourkova, G. Sadovska, Thermochim. Acta 452 (2007) 80.